Idelsohn *et al. Advanced Modeling and Simulation in Engineering Sciences(2022)9:22*
https://doi.org/10.1186/s40323-022-00235-7

Advanced Modeling and Simulation in Engineering Sciences

RESEARCH ARTICLE Open Access

The Pseudo-Direct Numerical Simulation Method considered as a Reduced Order Model

Sergio R. Idelsohn[1,2*], Juan M. Gimenez[1,3] and Norberto M. Nigro[3]

*Correspondence: sergio@cimne.upc.edu
[1]Centre Internacional de Mètodes Numèrics en Enginyeria (CIMNE), Barcelona, Spain
[2]Catalan Institution for Research and Advanced Studies (ICREA), Barcelona, Spain
[3]Centro de Investigación de Métodos Computacionales (CIMEC), Santa Fe, Argentina

Abstract

The multiscale method called Pseudo-Direct Numerical Simulation (P-DNS) is presented as a Reduced Order Model (ROM) aiming to solve problems obtaining similar accuracy to a solution with many degrees of freedom (DOF). The theoretical basis of P-DNS is other than any standard ROM. However, from a methodological point of view, P-DNS shares the idea of an offline computation, as ROM does, providing the set of coefficients, as a database or table, needed to solve the main problem. This work highlights the advantages and disadvantages of both methodologies. In particular, the drawback of the standard ROM concerning problems where space and time are not separated variables is discussed. The so-called Idelsohn's benchmark is possibly the most elemental test that can be proposed to point out this drawback. This one-dimensional heat transfer problem with a moving heat source shows that, unlike ROMs, P-DNS can solve it by reducing the number of degrees of freedom as much as needed.

Keywords: Reduced Order Models, Pseudo direct numerical simulation, Transient advection diffusion reaction problems, Idelsohn's benchmark, Multi-scale methods

Introduction

Today, numerical simulation is a standard tool in engineering. It is used for prediction and decision making, or simply for a better understanding of a particular physical phenomenon. Usually, in particular industrial applications, normally 2D or 3D with very complex geometries, a large number of degrees of freedom (DOF) are needed to obtain an accurate representation of current scenarios. Although classical methods are the standard to solve such problems, their significant computational effort precludes getting fast answers. Therefore, alternative numerical approaches are required. One of them is the Reduced Order Models (ROM).

ROM take advantage of the fact that the response of complex models can be often approximated, with reasonable precision, by the output of a surrogate model, seen as the projection of the initial problem on a lower-dimensional functional basis [1–3]. A classical categorization of ROM distinguishes *a posteriori* from *a priori* methods:

- The *a posteriori* methods are built after calculating solutions of the problem. The most classical example is the Proper Orthogonal Decomposition (POD) method [4–7], which is based on a statistical procedure called Principal Component Analysis (PCA).
- The *a priori* methods are constructed without the need to compute any solution to the problem. However, avoiding the calculation of snapshots implies the need to solve a sequence of nonlinear problems. A representative example of this type of method is Proper Generalized Decomposition (PGD) [8–13]. This method assumes, as a basic principle, that the solution of the governing equation can be approximated by a finite sum of the product of functions depending only on one variable.

Regardless of the strategy to obtain the modes, ROM assume that the problem requires a small number of modes to achieve an acceptable solution. If this is not the case, ROM have no advantage in solving the problem. From a methodological point of view, ROM proceed following two clearly defined operations: (1) the calculation of the base modes to be used, an operation that can be performed online in the case of a posteriori methods or offline, in the case of a priori methods, and (2) the solution of the problem in the obtained reduced base.

On the other hand, the recently presented multiscale method P-DNS (for Pseudo-Direct Numerical Simulation) [14–16] reduces the solution to a few degrees of freedom, problems which require a large number of degrees of freedom to be acceptably represented.

The theoretical basis of P-DNS is other than any standard ROM. In effect, the P-DNS method solves a problem by viewing it as a multiscale problem. The solution is computed on a relatively coarse scale, taking into account the contribution of a finer scale separately. However, from a methodological point of view, it shares the same target as ROM. Indeed, P-DNS solves with a few degrees of freedom, i.e. few unknowns at the coarse scale problem, reaching similar precision to a single scale solution considering many DOF.

Both methodologies require the computation of a series of parameters that, in many cases, is done offline. ROM needs the evaluation of the modes, while the P-DNS method demands calculating specific terms added by the fine scale in a representative volume element (RVE) by means of a fine mesh.

In this way, both methodologies can manage the large number of DOF needed to solve many current problems of the industry. However, as will be shown later in this work, the P-DNS method has a major advantage because it considers the degrees of freedom of both the fine and the coarse-scale. In particular, the DOF of the fine-scale are taken into account through the terms of the equations evaluated offline. On the other hand, ROM supposes that many base modes, fundamentally the high-frequency ones, do not participate in the solution and, therefore, are eliminated. For this reason, if all or a large number of modes are required to represent the solution, ROM find a severe obstacle turning impossible to reduce the number of degrees of freedom.

Another different use of ROMs is the one carried out in multiscale methods, when the scales are very different from each other [17]. In these methodologies, the model is treated as two separated models, where the fine scale is solved in a Representative Volume Element (RVE) using a ROM. In this way, the efficiency of the fine scale solution is improved. P-DNS also takes these ideas of multiscale methods and the separation of the fine-scale in RVEs. But the scales do not need to be different from each other. The main originality

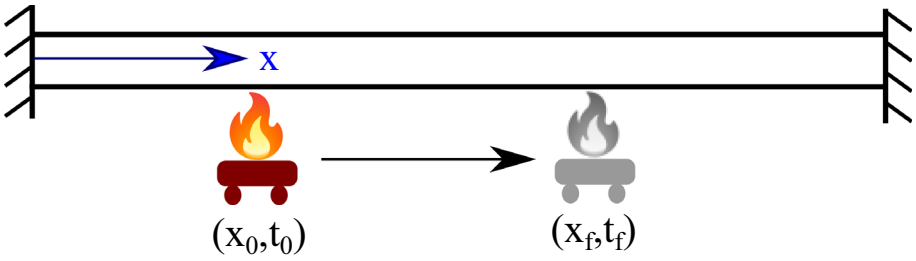

Fig. 1 Schematic representation of the Idelsohn's benchmark

is that the fine scale is solved offline, through a parametrization of the variables, which allows significantly increase of the computational efficiency of the coarse scale solution compared with the use of a ROM only in the fine scale.

Many of the problems which demand great number of base modes are those in which no separation variables in space and time is possible. In this sense, one of the simplest problem to be solved is the so-called Idelsohn's benchmark [18, 19], a one-dimensional heat transfer problem with a moving source (see Fig. 1). In this case, the existing drawbacks in the ROM are reflected. Moreover, this test will be used to show that, unlike ROM, P-DNS can solve it by reducing the number of degrees of freedom as much as needed.

In summary, the main idea behind this article is to consider P-DNS as another ROM method with some additional capabilities to deal with transient problems where space and time cannot be considered as separate variables. As a consequence of this objective, some particular novelties in P-DNS applied to unsteady problems, crucial to face such problems, are presented.

The organization of this paper is as follows: after a brief description of the P-DNS method for advection–diffusion–reaction problems, the approach is generalized for transient problems including those with a space-time variable source. The Idelsohn's benchmark will be solved by reducing orders in the number of DOF comparing the different solutions from some recent ROM references. Finally, to show all the advantages of the proposed P-DNS method, other transient advection–diffusion–reaction problems are computed by reducing the number of DOF.

The Pseudo-Direct Numerical Simulation method for advection-diffusion-reaction problems

Next, a summary is given about the P-DNS method applied to problems of advection, diffusion and reaction (ADR) one-dimensional, stationary, without internal source. A complete development of P-DNS for n-dimensional problems and vector equations (Navier–Stokes) can be found in the references [14].

Actually, the numerical solution of the stationary 1D ADR problem without an internal source has no real gain, since there is an analytical solution for this problem. However, it is useful to understand the method and generalize to problem in which no analytical solution is possible.

The equation to solve is

$$-\frac{d}{dx}\left(k\frac{dT}{dx}\right)+u\frac{dT}{dx}+rT=0 \tag{1}$$

where T is the unknown scalar variable of the problem, k is the diffusivity coefficient that will be considered constant and positive, u is an advection velocity of the material that will be considered constant, positive or negative, and r is a constant coefficient representing a reaction/absorption phenomenon that can also be positive or negative.

The boundary conditions are

$$T = \overline{T}, \text{ or } -k\frac{dT}{dx} = \overline{q} \text{ at } x = 0 \text{ and } x = L \tag{2}$$

being $\overline{T}$ and $\overline{q}$ known constant values for the Dirichlet and the Neumann boundary conditions.

Considering a Galerkin FEM-type approximation with linear shape and weighting functions $N(x)$, the equation to be solved, after a standard integration by parts, reads

$$\sum_{e=1}^{nel} \int_{H_e} \left[\frac{dN_i^e}{dx} \left(k\frac{dT}{dx} - uT \right) + N_i^e rT \right] dx = 0 \tag{3}$$

where the sum is made over the *nel* elements of length H_e and the shape functions of each element, considering the linear case with local coordinates centered at $x = 0$, are:

$$N_1^e = \left(\frac{1}{2} - \frac{x}{H_e} \right) \text{ and } N_2^e = \left(\frac{1}{2} + \frac{x}{H_e} \right) \qquad \text{with } x \in [-H_e/2, H_e/2]. \tag{4}$$

As previously stated, the idea of P-DNS is to split the unknown T into a coarse scale, called T_c, and a fine-scale, which will be called T_f. The idea is that the sum of both is a continuous but completely arbitrary function. However, certain restrictions on both functions, T_c and T_f, are imposed without violating the arbitrariness of the sum of them. Thus, T_c is considered the standard FEM approximation in a coarse mesh with elements of dimension H_e. In a given element, we define the coarse field as

$$T_c = T_c(x = 0) + Gx \text{ with } G = \frac{dT_c}{dx}. \tag{5}$$

On the other hand, it will be imposed on T_f in each element the following restriction:

$$T_f \left(x = -\frac{H_e}{2} \right) = T_f \left(x = \frac{H_e}{2} \right) = 0 \tag{6}$$

which implies that the integral of the derivative of T_f in each element satisfies:

$$\int_{H_e} \frac{dT_f}{dx}\, dx = 0. \tag{7}$$

As can be seen, these constraints maintain the arbitrariness of the sum function T. Incorporating this split into Eq. (3) the contribution of each coarse element to the sum is

$$\int_{H_e} \left[\frac{dN_{ci}}{dx} \left(k\frac{d(T_c + T_f)}{dx} - u(T_c + T_f) \right) + N_{ci} r(T_c + T_f) \right] dx = 0 \tag{8}$$

where for simplicity, we have isolated an arbitrary element of the coarse mesh and called N_{ci} the two weight-functions of that element. For the fine scales the equation to be solved is

$$\sum_{j=1}^{nelf}\left\{\int_h\left[\frac{dN_{fj}}{dx}\left(k\frac{d(T_c+T_f)}{dx}-u(T_c+T_f)\right)+N_{fj}r(T_c+T_f)\right]dx\right\}=0 \tag{9}$$

where the coarse element has been subdivided in *nelf* elements of dimension h being N_{fj} the weight-functions corresponding to the fine-scale.

The other main idea of P-DNS is to solve the Eq. (9) offline, only once, for a dimensionless element that can represent all the possible configurations that can occur in this problem. In this particular case, this Representative Volume Element (RVE) is considered coincident with an element of the coarse mesh. However, as can be seen in other P-DNS publications [14–16], an RVE has not necessarily a one-to-one correspondence with an element of the coarse mesh.

After imposing the restrictions (5), (6), and (7) the Equation of the coarse scale (8) remains

$$\int_{H_e}\left[\frac{dN_{ci}}{dx}\left(k\frac{dT_c}{dx}-uT_c\right)+N_{ci}rT_c\right]dx+\underbrace{\int_{H_e}\left[-\frac{dN_{ci}}{dx}uT_f+N_{ci}rT_f\right]dx}_{-\frac{dN_{ci}}{dx}u\int_{H_e}T_f\,dx+r\int_{H_e}N_{ci}T_f\,dx}=0 \tag{10}$$

where can be seen that, according to N_{ci}'s definition, the only terms needed to be known from the fine scale are

$$\tau=\int_{H_e}T_f\,dx\ \text{, and}\quad \tau_x=\int_{H_e}xT_f\,dx. \tag{11}$$

As previously stated, the fine scale problem, see Eq. (9), is solved offline only once and forever, for a dimensionless RVE, preserving the following dimensionless variables,

$$\mathrm{Pe}^{H_e}=\frac{uH_e}{k},\ \text{and}\ \mathrm{w}^{H_e}=\frac{rH_e^2}{k} \tag{12}$$

obtained after using the following non-dimensional definitions for the variables involved:

$$\hat{T}=\frac{T}{T_M};\hat{H}=\frac{H}{H_e};\hat{G}=\frac{GH_e}{T_M};\hat{x}=\frac{x}{H_e};\hat{\tau}=\frac{\tau}{T_MH_e};\hat{\tau_x}=\frac{\tau_x}{T_MH_e^2};\hat{f}=\frac{fH_e^2}{kT_M} \tag{13}$$

where the symbol $\hat{}$ indicates a dimensionless quantity, T_M is the average value of the unknown inside each element and f is an external source.

In Fig. 2 a graphical description of what the whole process is presented, although as will be seen later, the final methodology is modified in order to make it efficient. P-DNS uses a multiscale approach where the global problem is solved on a coarse mesh. The fine scales are solved in separate problems, where for each coarse element e, a particular problem with $(\mathrm{Pe}^{H_e}, \mathrm{w}^{H_e})$ is solved with boundary conditions given by the coarse scale field T_c.

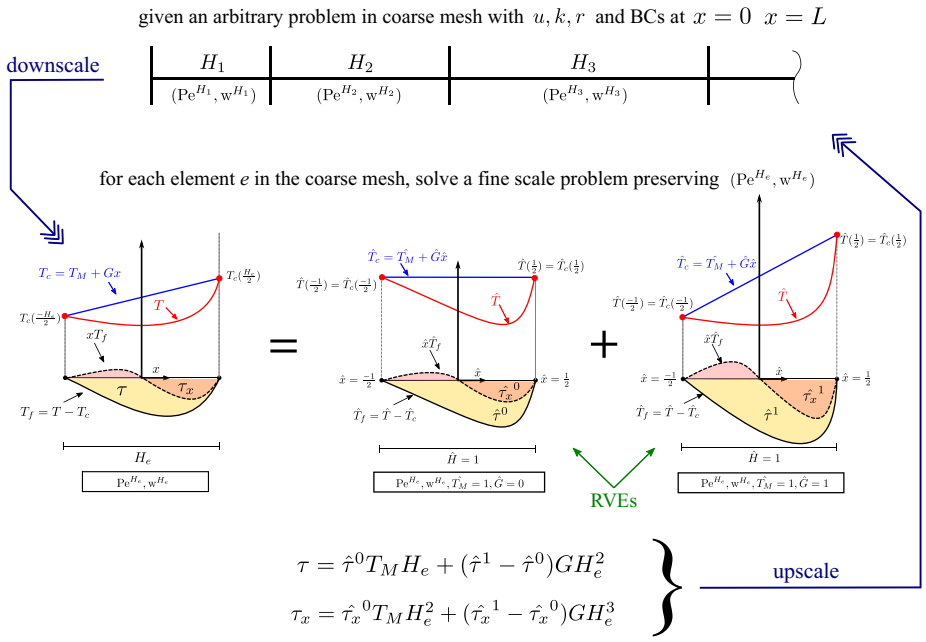

Fig. 2 A graphical description of the general idea in the P-DNS methodology for solving an arbitrary ADR problem. Due to the linearity of the problem, the superposition theorem allows splitting the fine scale into two canonical problems

Each of these fine scale problems differ in the dimensionless numbers that reign and also the boundary conditions to apply dictated by the coarse solution through its nodal values, i.e. its mean value and its first derivative. In order to make the computation efficient, it is a matter of bringing all these problems to the same reference domain, the RVE, of arbitrary size, seeking to minimize the number of computations necessary to cover all the different situations that occur in the coarse mesh. In addition, due to the linearity of the problem, the superposition theorem can be applied. Every combination of the different averages and slopes can be represented by only two cases with an average value of unit value for the dimensionless variable, i.e. $\hat{T_M} = 1$, and $\hat{G} = 0$ or $\hat{G} = 1$ for the slope. Finally a scaling with the current mean value and slope of each coarse element is done.

Therefore, the value of $\hat{\tau}$ and $\hat{\tau_x}$ for an arbitrary $\hat{G}$ can be evaluated as:

$$\hat{\tau} = \hat{\tau}^0 + (\hat{\tau}^1 - \hat{\tau}^0)\hat{G}, \tag{14a}$$

$$\hat{\tau_x} = \hat{\tau_x}^0 + (\hat{\tau_x}^1 - \hat{\tau_x}^0)\hat{G} \tag{14b}$$

and then using Eq. (13)

$$\tau = \hat{\tau} T_M H_e = \left[\hat{\tau}^0 + (\hat{\tau}^1 - \hat{\tau}^0)\hat{G}\right] T_M H_e = \hat{\tau}^0 T_M H_e + (\hat{\tau}^1 - \hat{\tau}^0) G H_e^2, \tag{15a}$$

$$\tau_x = \hat{\tau_x} T_M H_e^2 = \left[\hat{\tau_x}^0 + (\hat{\tau_x}^1 - \hat{\tau_x}^0)\hat{G}\right] T_M H_e^2 = \hat{\tau_x}^0 T_M H_e^2 + (\hat{\tau_x}^1 - \hat{\tau_x}^0) G H_e^3 \tag{15b}$$

Each one of the fine scale problems generates a solution in the RVE that allows computing the response of the fine scales (τ, τ_x) to upscale to the coarse mesh. The process ends when the contribution of the fine scales is introduced as source terms over the coarse scale problem as shown in Eq. (10).

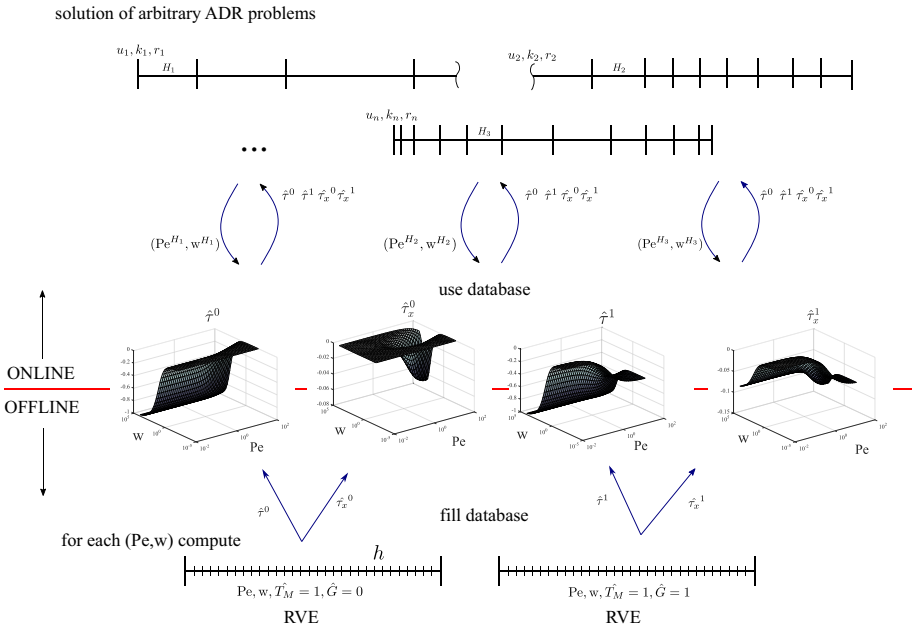

Fig. 3 A graphical description of the actual P-DNS methodology for 1D ADR problems. To fill the database, $N_{\mathrm{Pe}} \times N_{\mathrm{w}} \times 2$ RVE problems were solved. This offline work is done once and used online to solve any coarse scale 1D ADR problem

Instead of carrying out the entire process on the fly, an a priori and offline stage is proposed for the preparation of a database. This latter is a table which serves for the online consulting using as input the dimensionless pair (Pe, w). The outputs are four dimensionless values ($\hat{\tau}^0$, $\hat{\tau}^1$, $\hat{\tau_x}^0$, $\hat{\tau_x}^1$), the integrals represented by Eq. (11), that enable computing the dimensional τ and τ_x using Eq. (15). The number of RVE solutions required to build this database, once a time and for any ADR problem, is proportional to $N_{\mathrm{Pe}} \times N_{\mathrm{w}} \times 2$ being N_{Pe} and N_{w} the number of samples used to discretize the range of the dimensionless inputs. Each of these problems is solved on the RVE domain of total length $\hat{H} = 1$ discretized with a mesh as fine as accuracy needs.

The Fig. 3 shows the actual P-DNS methodology applied to arbitrary one-dimensional ADR problems. The *online* work is shown at the top, which includes the entire set of ADR problems that could be posed, each one represented by the advection, diffusion and reaction coefficients plus the coarse mesh discretization. At the bottom, the *offline* work done once and for all to fill the database associated with generic ADR problems.

Replacing the values obtained in Eqs. (15a) and (15b) in the Equation of the coarse scale (10), the solution to the ADR problem at the coarse scale is calculated. This solution presents the same precision as the one obtained if the problem were solved with a mesh as fine as the one we used to solve the RVE offline, with the consequent saving in time and memory. In the ADR case, the analytical solution of the RVE problem is known. By using that solution to compute the RVE outputs, the exact result at machine precision would have been obtained, regardless of the number of elements used in the coarse mesh. This is an ideal case to check the validity of this methodology. However, this situation is lost if more spatial dimensions are included and in consequence the RVE mesh size should be adapted to the accuracy needed.

It is interesting to emphasize that the possibility of obtaining, in a post-process step, the value of the solution at any location in the coarse mesh is another advantage of the P-DNS method. In fact, it is enough to evaluate, when the offline RVE is processed, the value of the unknown function at any predetermined interior point $\hat{x}_i$. For example, let $\hat{T}^0(\hat{x}_i)$ and $\hat{T}^1(\hat{x}_i)$ be the values of $\hat{T}$ evaluated in the RVE for the case of $\hat{G}=0$ and $\hat{G}=1$, respectively. Then, the value of the function $T(x_i)$ at any interior point x_i is equal to

$$T(x_i) = \hat{T}^0(\hat{x}_i)T_M + \left[\hat{T}^1(\hat{x}_i) - \hat{T}^0(\hat{x}_i)\right] GH_e. \tag{16}$$

It is necessary to highlight that the number of outputs of the database is not a dimensional limitation as the number of inputs. Each new input implies adding a new dimension to the parameter space increasing significatively the combination of different cases to be solved in the RVE. This is not the case for the number of outputs. The number of inputs involved is always equal to two for ADR problems.

As the main conclusion for the ADR case, it can be said that: once a database is built, it has as input Pe and w and has as output the four values of $\hat{\tau}^0$, $\hat{\tau}^1$, $\hat{\tau_x}^0$ and $\hat{\tau_x}^1$, and eventually the values of $\hat{T}^0(\hat{x}_i)$ and $\hat{T}^1(\hat{x}_i)$ at some interior points. Using this database, any arbitrary 1D ADR problem, stationary and without an external source, can be solved for any mesh, including the particular case of a single element in the whole domain. The accuracy depends exclusively on the number of elements used when solving the RVE. As the analytical solution of the ADR problem is known in the RVE, the exact solution can be obtained in all cases, regardless of the mesh used to solve the coarse problem.

Generalization to transient problems and/or problems with a variable source in space/time

The equation to solve for the 1D transient advection-diffusion-reaction problem with source (TADRS) becomes

$$\rho C_p \left(\frac{\partial T}{\partial t} + u\frac{\partial T}{\partial x}\right) - \frac{\partial}{\partial x}\left(k'\frac{\partial T}{\partial x}\right) + r'T = f'(x,t) \tag{17}$$

where ρ is the density, C_p is the specific heat and f' is an arbitrary source term depending on x and t. Here the thermal problem is chosen but the same is valid for any scalar transport equation.

Dividing all the equation by ρC_p, the equation is written as

$$\frac{\partial T}{\partial t} + u\frac{\partial T}{\partial x} - \frac{\partial}{\partial x}\left(k\frac{\partial T}{\partial x}\right) + rT = f(x,t) \tag{18}$$

where now the physics coefficients k and r as well as the source term are defined as: $k = \frac{k'}{\rho C_p}$, $r = \frac{r'}{\rho C_p}$ and $f = \frac{f'}{\rho C_p}$. It is true that respecting the P-DNS philosophy, the space-time domain could be split into a coarse space-time plus a fine space-time scale. However, in this work, the temporal part of Eq. (18) is integrated by any first or second-order approximation. The errors that this integration introduces, which depend on the time step (Δt) adopted, are not intended to be eliminated in this work. Therefore, the result will be no longer exact as before because it will incorporate the errors that are inherent to the temporal approximation.

Let consider that at time $t = t^{n+\theta}$, the time derivative of the unknown is

$$\left.\frac{\partial T}{\partial t}\right|^{n+\theta} = \frac{T^{n+1} - T^n}{\Delta t} \tag{19}$$

which is exact for some unknown value of θ and a given $\Delta t = t^{n+1} - t^n$. Furthermore, the value of the unknown in any time inside the interval Δt will be considered with a linear variation in time.

$$T^{n+\theta} \approx \theta T^{n+1} + (1-\theta)T^n. \tag{20}$$

With these approximations, the semidiscrete in time version of Eq. (18) remains the following ordinary differential equation (ODE)

$$\begin{aligned}&\frac{T^{n+1} - T^n}{\Delta t} + \theta u \frac{dT^{n+1}}{dx} - \frac{d}{dx}\left(\theta k \frac{dT^{n+1}}{dx}\right) + \theta r T^{n+1} \\ &= f^{n+\theta}(x) - (1-\theta)u\frac{dT^n}{dx} + \frac{d}{dx}\left((1-\theta)k\frac{dT^n}{dx}\right) - (1-\theta)rT^n,\end{aligned} \tag{21}$$

which assumes that T^n is known from the previous time step and that the only unknown is T^{n+1}. Gathering the physical and numerical constants, the ODE can be rewritten as

$$u\frac{\partial T}{\partial x} - \frac{\partial}{\partial x}\left(k\frac{\partial T}{\partial x}\right) + cT = F \tag{22}$$

where for simplicity we define $k \leftarrow \theta k$; $u \leftarrow \theta u$; $c = \theta r + \frac{1}{\Delta t}$, $T \leftarrow T^{n+1}$, and

$$F(x) = f^{n+\theta}(x) - (1-\theta)u\frac{\partial T^n}{\partial x} + (1-\theta)\frac{\partial}{\partial x}\left(k\frac{\partial T^n}{\partial x}\right) - \left[(1-\theta)r - \frac{1}{\Delta t}\right]T^n. \tag{23}$$

From the point of view of P-DNS, the strategy to solve each time step is similar to the solution of the previous ADR problem. The only difference is that now a modified reactive term and a spatially variable source function must be considered. This source function depends on the solution of the previous time step and on the external source itself, if any. The introduction of an arbitrary spatially variable source function is not a problem for the multiscale strategy of P-DNS, but it is a problem for the offline solution strategy using a unique RVE to solve the fine scale. This drawback is overcome by approximating the source $F(x)$ with as many piecewise linear functions of the same type as those used in FEM as necessary to reproduce its spatial variation with acceptable precision. Also it may be considered the usage of globally defined higher order polynomials.

Then be

$$F(x) \approx F_F(x) = \sum_{i=0}^{np-1} N_i^F F(x_i^F) \tag{24}$$

where np is the number of points used to discretize $F(x)$; N_i^F are the shape functions used and x_i^F the position of the points.

Applying the spatial splitting into coarse and fine solutions, replacing in Eq. (22), and weighting with the coarse shape functions, the same left hand side of Eq. (10) is get. This

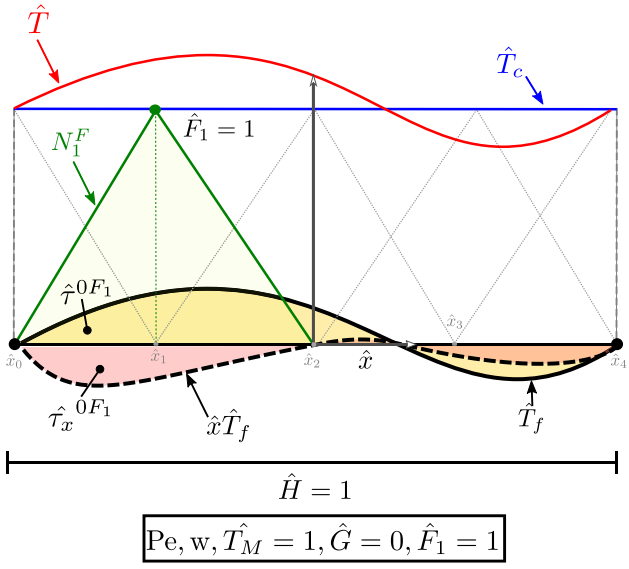

Fig. 4 The functions to be evaluated offline in an RVE. It considers the case $i = 1$ for a discretization of $np = 5$ for the source. For a given Pe and w, and additionally to the cases presented in Fig. 2, np RVE problems must be computed. The integral $\hat{\tau}^{0F_i}$ and the first moment $\hat{\tau_x}^{0F_i}$ of the fine solution $\hat{T}_f$ are stored in the database

means the contribution of the fine scales to the coarse problem is restricted to compute the integrals given by Eq. (11). Meanwhile, the right hand side remains

$$\int_{H_e} N_{ci} F(x)\, dx \approx \int_{H_e} N_{ci} \sum_{i=0}^{np-1} N_i^F F(x_i^F)\, dx. \tag{25}$$

Considering Eq. (23), it is evident the need for storing previous values of the unknown, i.e. T_c^n and T_f^n, to compute $F(x)$.

At the RVE level, taking into account the linearity of the problem, the dimensionless integrals $\hat{\tau}$, and $\hat{\tau_x}$ should be redefined. The fine scale solution must consider a fictitious distributed load equal to each of the shape functions used to discretize the source, see Fig. 4. Calling with $\hat{\tau}^{0F_i}$ and $\hat{\tau_x}^{0F_i}$ each of these integrals, the total value of the integrals $\hat{\tau}$ and $\hat{\tau_x}$ is obtained by adding each product of the integral obtained at the RVE level by the value of current source function at each point.

$$\hat{\tau} = \hat{\tau}^0 + (\hat{\tau}^1 - \hat{\tau}^0)\hat{G} + \sum_{i=0}^{np-1} (\hat{\tau}^{0F_i} - \hat{\tau}^0)\hat{F}(x_i) \tag{26a}$$

$$\hat{\tau_x} = \hat{\tau_x}^0 + (\hat{\tau_x}^1 - \hat{\tau_x}^0)\hat{G} + \sum_{i=0}^{np-1} (\hat{\tau_x}^{0F_i} - \hat{\tau_x}^0)\hat{F}(x_i). \tag{26b}$$

Using the Eq. (13) to go from the dimensionless variable to the real one, the following value for the integrals τ and τ_x are obtained

$$\tau = \hat{\tau}^0 T_M H_e + (\hat{\tau}^1 - \hat{\tau}^0) G H_e^2 + \frac{H_e^3}{k} \left[\sum_{i=0}^{np-1} (\hat{\tau}^{0F_i} - \hat{\tau}^0) F(x_i) \right] \tag{27a}$$

$$\tau_x = \hat{\tau_x}^0 T_M H_e^2 + (\hat{\tau_x}^1 - \hat{\tau_x}^0) G H_e^3 + \frac{H_e^4}{k} \left[\sum_{i=0}^{np-1} (\hat{\tau_x}^{0F_i} - \hat{\tau_x}^0) F(x_i) \right] \tag{27b}$$

In the same way, the evaluation a local value of the unknown function in an arbitrary internal point x_j must be modified. Now it is necessary to compute during the RVE evaluation, in addition to those already defined $\hat{T}^0(\hat{x}_j)$ and $\hat{T}^1(\hat{x}_j)$, the value of $\hat{T}^{0F_i}(\hat{x}_j)$. Then, the value of the unknown in the internal point x_j is

$$T(x_j) = \hat{T}^0(\hat{x}_j) T_M + \left(\hat{T}^1(\hat{x}_j) - \hat{T}^0(\hat{x}_j) \right) G H_e + \frac{H_e^2}{k} \left[\sum_{i=0}^{np-1} \left(\hat{T}^{0F_i}(\hat{x}_j) - \hat{T}^0(\hat{x}_j) \right) F(x_i) \right] \tag{28}$$

Equations (27a) and (27b) are used to evaluate the terms needed in Eq. (10), to solve one time step of the TADRS problem. Furthermore, Eq. (28) is used to evaluate the unknown function in some internal points.

Now in TADRS problems, the evaluation of internal points of the unknown is not optional. Now, this evaluation is needed to approximate the unknown in the previous time steps, which are required to calculate part of the function F, as seen in Eq. (23). Indeed, at each time step, it is necessary to evaluate and save for the next time step unless the value of the unknown $T^{n+1}(x_j)$ at as many interior points as used to discretize F.

Building the TADRS database. In Fig. 5 the P-DNS methodology applied to TADRS problems in depicted. In TADRS problems, the dimensionless inputs to the database are, as before in the ADR case, two values, Pe and w. But now, the dimensionless outputs of the database are: a) the same four coefficients as before ($\hat{\tau}^0$, $\hat{\tau}^1$, $\hat{\tau_x}^0$, $\hat{\tau_x}^1$), plus two coefficients for each one of the np points needed to correctly represent the function F, i.e. $\hat{\tau}^{0F_i}$ and $\hat{\tau_x}^{0F_i}$; b) in addition, for the evaluation of the values of the unknown function in interior points j, the same two previously values are needed, $\hat{T}^0(\hat{x}_j)$ and $\hat{T}^1(\hat{x}_j)$, plus one more coefficient for each interior point added, i.e. $\hat{T}^{0F_i}(\hat{x}_j)$.

For each pair of inputs (Pe_i,w_i) a set of 1D ADRS problems must be solved to compute the output coefficients. These solutions are computed in the RVE using a very fine mesh to reduce the approximation errors. In this work, a grid size $h^f = 0.0005$ is selected after a convergence analysis where for finer meshes the changes in the uploading variables is below a given tolerance. To guarantee the second-order discretization using linear finite elements, the local restrictions of $\mathrm{Pe}^{h^f} \leq 1$ and $\mathrm{w}^{h^f} \leq 1$ are accomplished for stability reasons adding local refinement when necessary.

Figure 5 presents the variation of the dimensionless RVE outputs ($\hat{\tau}^0$, $\hat{\tau}^1$, $\hat{\tau_x}^0$, $\hat{\tau_x}^1$) versus the dimensionless input numbers Pe and w. In particular, the database shown was constructed with 1271 RVE simulations ranging Pe from 10^{-2} to 10^2, and w from 10^{-5} to 10^5, with a logarithmic distribution of the samples.

Additionally, Fig. 5 presents the variation of some of the dimensionless RVE outputs that accounts for the influence of the source on the solution, i.e. $\hat{\tau}^{0F_i}$ and $\hat{\tau_x}^{0F_i}$ regarding Pe and w. The outputs displayed are for the cases $i = 0$ and $i = 1$ when the number of points used to discretize the source is $np = 2$.

In order to evaluate the sensitivity and convergence of the coarse scale solution regarding the number of points used to discretize the source, we have constructed as many databases

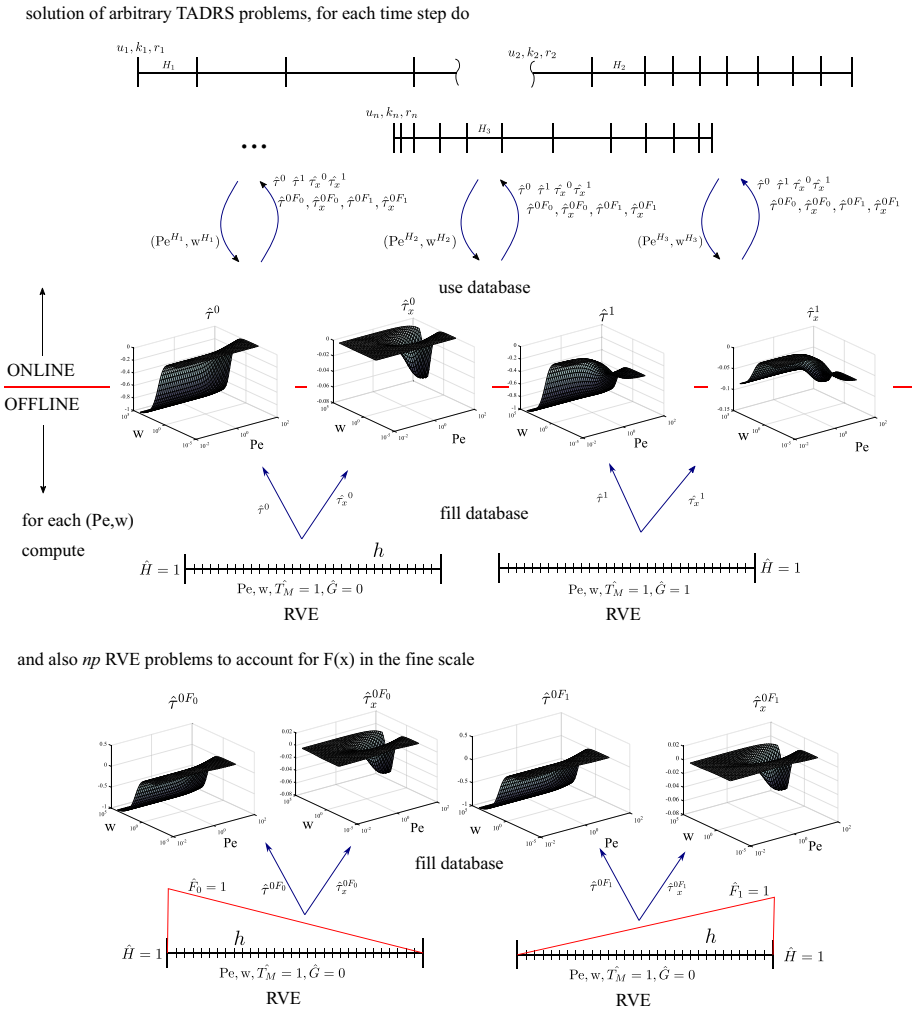

Fig. 5 A graphical description of the actual P-DNS methodology for 1D TADRS problems. To fill the database, $N_{\text{Pe}} \times N_{\text{w}} \times (2 + np)$ RVE problems were solved. This offline work is done once and used online to solve any 1D TADRS coarse scale problem. In this example, the number of points to discretize the source is $np = 2$

as the different *np* values we need in the following Sections. In the view of the results obtained, we will conclude this work giving an advice about the proper selection of *np*.

Finally, the steps to employ the database in a given mesh element of the coarse scale consists in:

(a) evaluate the dimensionless inputs, Eq. (12),
(b) predict the fine-scale response using the information provided by the database,
(c) re-scale the output coefficients, Eq. (13).

In step (b), interpolation should be carried out to determine the outputs for arbitrary Pe and w values. The ability to represent the nonlinear variation of the outputs is crucial to obtain accurate coarse mesh solutions [15].

The solution of the Idelsohn's benchmark via the P-DNS method seen as ROM

A classical example of non-separable problems was established in a joint Spanish-French workshop held at Jaca, Spain, in 2013. The definition of the benchmark is the following: a transient problem is defined on a one-dimensional domain $x = [0, L]$, over the time

interval $t = [0, t_{end}]$. It is assumed that a prescribed zero temperature is applied on $x = 0$ and $x = L$ and that the domain is subjected to a time-dependent thermal loading that consists of a thermal source $f(x, t)$. This loading can be seen as a moving flame/laser beam such that $f(x, t) = \delta(x - vt)$ a Dirac distribution, where v is the velocity of the flame/laser beam (see Fig. 1). For the sake of simplicity, the initial conditions are set to zero. The material is assumed to be homogeneous and fully known where k represents the heat capacity and ρC_p the density by the specific heat parameter of the material. The example was nominated as the *Idelsohn's benchmark* in [18,19]. The problem has been solved by applying POD and PGD in their global, classical version. These results will serve as a reference for the degree of reduction attainable by another ROM.

Despite its simplicity, this benchmark represents a series of phenomena that appear in a large number of problems in the industry [20,21]. Take, for instance, the problems of welding, where a highly concentrated heat source is moving in different directions, the problems of cutting materials by laser and/or the very now fashionable methods of additive manufacturing, to name just a few of the phenomena directly related to the Idelsohn's benchmark.

Moreover, this test case represents a series of phenomena much larger than those related to moving concentrated sources. This case represents all the problems where the variables are inherently non-separable, as seen frequently in the industry. Indeed, some problems have, by definition, a solution structure that is inherently inseparable. According to the Fourier decomposition any function may be written as a sum of the product of separable functions, although the number of terms required can be really large. In this case, the variables are said to be intrinsically non-separable and these are the phenomena in which ROM is not capable of reducing the number of degrees of freedom of the set.

In order to see this drawback of the standard ROM, Fig. 6a represents the solution in space-time of the Idelsohn's benchmark for some particular coefficients. The FEM result with 150 linear elements, i.e. 149 degrees of freedom (DOF), is considered the *reference* or DNS solution of this problem. On the other hand, Fig. 6b represents the solution of the same problem using a standard POD. The solutions with 5, 10 and 20 DOF are insufficient as non-physical high frequencies are noticeable. At least 70 modes are needed to avoid these numerical artifacts and obtain a satisfactory solution. However, a reduction from 149 DOF to 70 DOF it is useless from a ROM's point of view.

The poor separability of the solution makes ROM global approaches incapable to find a suitable basis set in order to project the solution. To avoid these problems, the idea of local basis arises naturally. Initial works were done in the framework of POD-based methods and after were extended to PGD approaches [19]. However, these methodologies, in addition to the complication they introduce, are unfair since they make Idelsohn's benchmark loses its reason for being. The spirit of Idelsohn's benchmark is to find methods that, although the variables are not separable, work well and can be reduced.

Some solutions of the Idelsohn's benchmark using P-DNS are presented below. The difficulty of the problem depends largely on the source velocity. For zero velocity, the test becomes of separate variables and can be solved precisely with 4 or 5 POD modes. On the other hand, for high source velocity, the difficulty increases. Defining the dimensionless number $\mathrm{Pe} = vH_e/k$, for $\mathrm{Pe} \geq 1$, visible space-time coupling issues begin to be noticed. In this section we will deal with $\mathrm{Pe} \geq 1$.

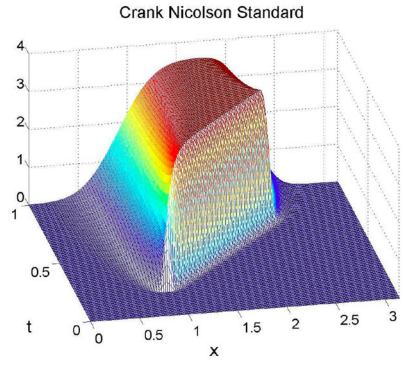

(a) FEM solution with 150 linear elements

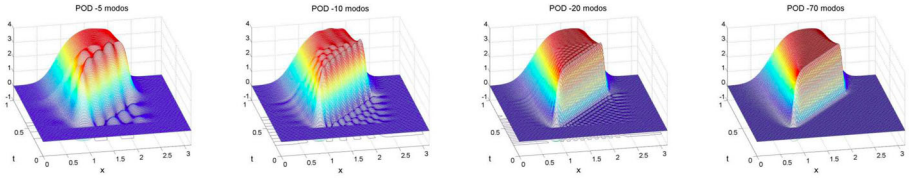

(b) Solution using 5, 10, 20 and 70 POD modes

Fig. 6 The Idelsohn's benchmark. Time–space solutions highlighting the drawbacks of global POD solutions

The configuration used defines a source $f(x, t)$ with high velocity v such as:

$$f(x,t) = \begin{cases} 0 & t < t_i \text{ or } t > t_f \\ A \cos \frac{\pi}{L}(x - x_0(t)) & t_i <= t \text{ and } -\frac{L}{2} < x - x_0(t) < \frac{L}{2} \end{cases} \tag{29}$$

where $x_0(t) = x_i + v(t - t_i)$, $A = 100$, $L = 0.15$, $t_i = 0.2$, $t_f = 0.7$, $x_i = \frac{2\pi}{7}$, $x_f = \frac{5\pi}{7}$, and $v = \frac{x_f - x_i}{t_f - t_i}$. The material is defined with $k = 0.05$ and $\rho C_p = 1$.

To analyze the results, the different approximation factors of the proposed P-DNS method must be taken into account. On one hand, there are the standard variables for any transitory problem, that are: (a) for the temporal approximation, the time-step and the θ coefficient used; and (b) for the spatial approximation, the number of elements used in the coarse mesh, which will give us the number of degrees of freedom of the problem. But, for P-DNS, there are other variables specific to the method that influence its precision. These are: (a) the number of points in each element used to approximate the source; and (b) the number of elements used in the fine mesh, that is, in the RVE built offline.

For the full order model (DNS) 300 linear elements were used with a $\Delta t = 0.00125s$ and $\theta = 1$. This gives a space-time reference solution T^{ref} of 300×800 sampling points. The P-DNS results presented in Fig. 7 are computed preserving the parameters for the temporal approximation and varying the number of elements used in the coarse mesh. In this case study, we use the database with a number of points to discretize the source $np = 26$. An analysis of the convergence will be made later as a function of np.

The relative error between an approximated solution T and the reference solution is the ratio between the error measured in energy norm, or L2-norm, and the energy norm of T^{ref}:

$$e = ||T - T^{ref}||_{L_2} \tag{30}$$

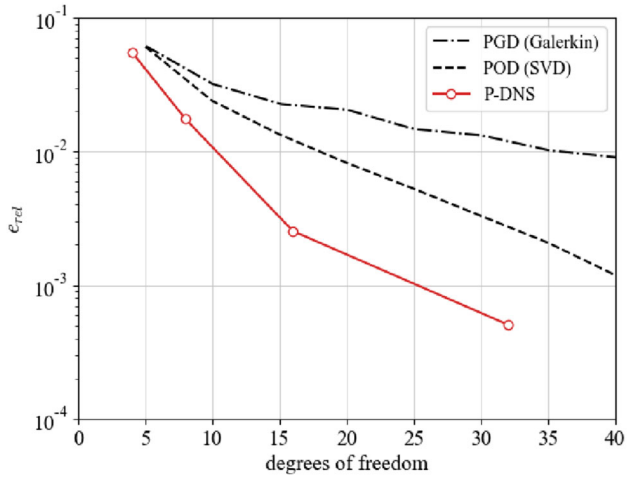

Fig. 7 The Idelsohn's benchmark. Relative error varying the degrees of freedom. In the case of ROM solutions, DOF is the number of modes. For P-DNS, DOF is the number of nodes of the coarse mesh

$$e_{rel} = \frac{e}{||T^{ref}||_{L_2}} \tag{31}$$

In the case of P-DNS, only the values of the solution on the nodes of the coarse mesh are considered to compute e.

The convergence curves are given in Fig. 7 for the relative error of P-DNS and selected global ROM approaches. The ROM solutions using PGD Galerkin and the optimum POD decomposition through the Singular Value Decomposition (SVD) are taken from [18]. To be able to compare the results, the concept of degrees of freedom is established as the number of modes employed in the ROM solutions, and as the number of elements of the coarse mesh used in the P-DNS calculations. Considering as target a relative error of 1%, P-DNS requires approximately 10 DOF to reach the required accuracy. Global ROM approaches requires more DOF: SVD more than 15 and PGD more than 30. Additionally the convergence rate with the number of modes is poor for the global PGD solutions, as reported previously.

Figure 8 presents snapshots of the solution of the Idelsohn's benchmark at different simulation times. The reference solution is compared with the P-DNS and the standard FEM solutions using a coarse grid of $nel = 8$ and a time-step such as the dimensionless source speed is $\hat{v} = \frac{v\Delta t}{\Delta x} = 0.2$. As shown, the P-DNS leads to accurate nodal results (bigger circles), but the coarse mesh solution could not be useful enough because the piece-wise linear interpolation widely misses the variation of the solution inside the elements. Therefore, we take advantage of the multiscale features of the P-DNS method, i.e. the physical behavior at a smaller scale can be introduced from pre-computed RVE results using Eq. (28). Then, we display the solution complemented with the values at the $np - 2$ interior points used to discretize the source (smaller circles).

Other solutions of transient advective–diffusive–reactive problems via the P-DNS method with different reduction order

Regardless of Idelsohn's benchmark, the P-DNS method has been tested in general in stationary and transient advection-diffusion-reaction problems with or without source.

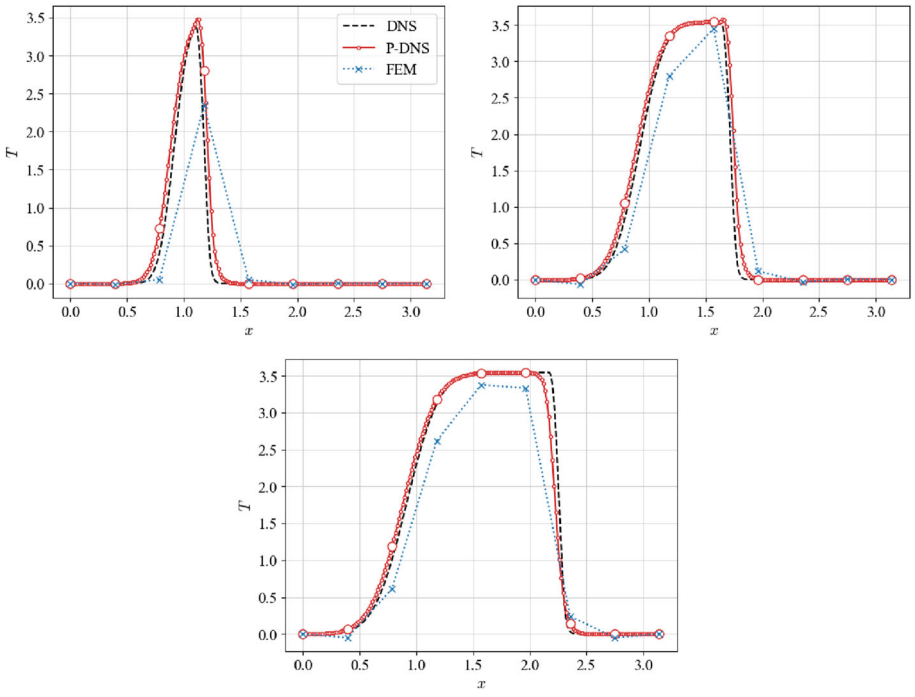

Fig. 8 The Idelsohn's benchmark. $\hat{v} = 0.2$ and $nel = 8$. Snapshots of the FEM and P-DNS solution for $t = 0.3$ s (top-left), 0.5 s (top-right) and 0.7 s (bottom) while compared with the DNS reference. For the P-DNS solution larger circles are the nodal values and smaller circles are the values on the *np* dicretization points of the source

An extension to two-dimensional ADR cases can be found in reference [15]. Likewise, for three-dimensional transient problems in vector equations such as the Navier–Stokes equations, can be found in references [14,16]. We will show here just some one-dimensional problems in which the P-DNS method can be considered as a ROM method.

Another aim of this Section is to evaluate the sensitivity and convergence of the coarse scale solution regarding the number of points used to discretize the source, *np*. Hereinafter, when a number of *np* is said to be selected, it means using the database where the source was discretized with *np* points.

Advection–diffusion–reaction with an exponential Source

The analysis domain is $\Omega \in [0,6]$ where a stationary advective–diffusive–reactive problem with an exponential Source (ADRS) is solved. The physical coefficients chosen are $u = 1$, $k = 0.1$ and $c = 2$. Dirichlet boundary conditions are imposed on the boundaries, such as $T(x = 0) = 3$ and $T(x = 8) = 8$. A source that varies exponentially with x as $f(x) = 0.1\exp(x)$ is established.

The exact solution of this problem is obtained using a symbolic library. This reference result is used to evaluate the prediction error of the numerical approximations. Figure 9 compares the exact solution with the numerical ones obtained using P-DNS and the standard FEM for homogeneous spatial discretizations of $nel = 2, 4$, and 8. The FEM solutions present the expected instabilities towards the boundary layer on the right when second order schemes for advective terms are employed and no stabilization is included. The P-DNS solutions, which were obtained using $np = 2$ to discretize the source, show a stable result.

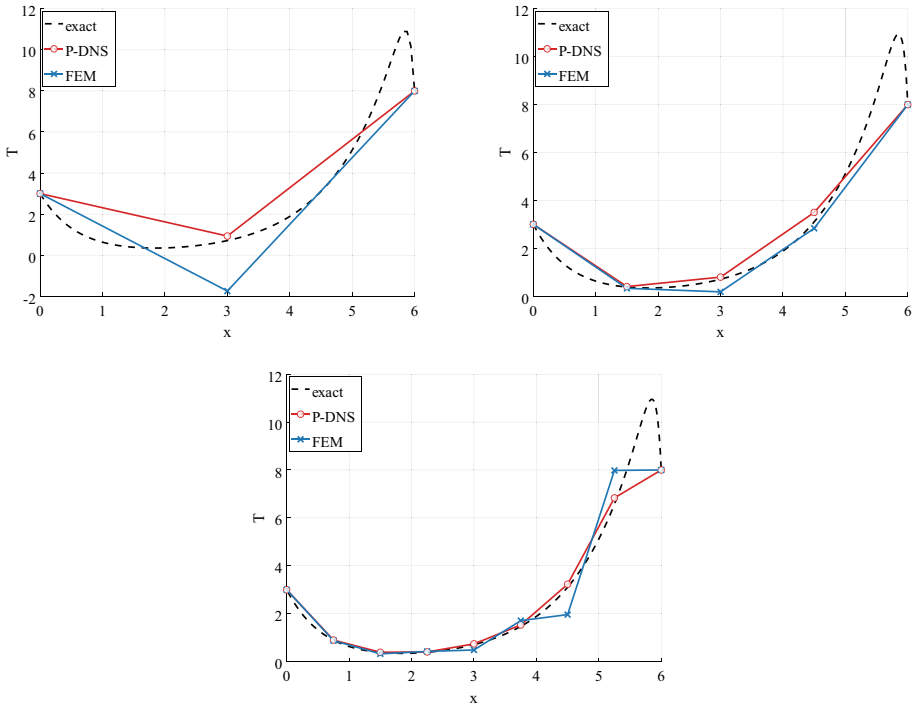

Fig. 9 Advection–diffusion–reaction with an exponential Source with $nel = 2$ (top-left), 4 (top-right), and 8 (bottom). Nodal results from FEM and P-DNS with $np = 2$ are compared with the exact solution

As the exponential source is represented through linear approximations, the P-DNS method does not yield the exact solution on nodal values. Therefore an analysis of the convergence of the error of P-DNS regarding the choice of *np*, the number of points per coarse element to discretize the source, is performed. Figure 10 presents the convergence of the numerical error when *nel*, the number of elements of the coarse mesh, is increased. After an initial phase of instability for coarse meshes, FEM attains the expected second-order convergence with spatial discretization. In general, the solutions with P-DNS shows lower absolute error. The error decreases quadratically with *nel* for any *np*. Then, the absolute error level can be tuned by the choice of *np*. For example, to reach an absolute error $e < 10^{-3}$, FEM requires employing a mesh of more than 256 elements. The ability of P-DNS of working as a ROM is also noticeable in this example because this multiscale method can achieve the same error level using, for example, only a mesh of 10 elements and $np = 11$.

A transient advective–diffusive–reactive problem

The analysis domain $\Omega \in [0, 8]$ is discretized into eight 2-node elements of equal length. The advection, diffusion and reaction coefficients are chosen as $u = 1$, $k = 0.1$ and $c = 2$. Using these data, the dimensionless numbers are Pe = 5, w = 170. Dirichlet boundary conditions are imposed on the boundaries, such as $T(x = 0) = 3$ and $T(x = 8) = 8$. The initial solution is a linear profile. The transient solution is obtained using an implicit time integration with $\theta = 0.5$. Figure 11 shows the solution obtained considering different time steps where the results using the P-DNS method with $nel = 8$ and $np = 26$ with $\Delta t = 0.125$ s are compared with a DNS solution. The latter was obtained by solving the

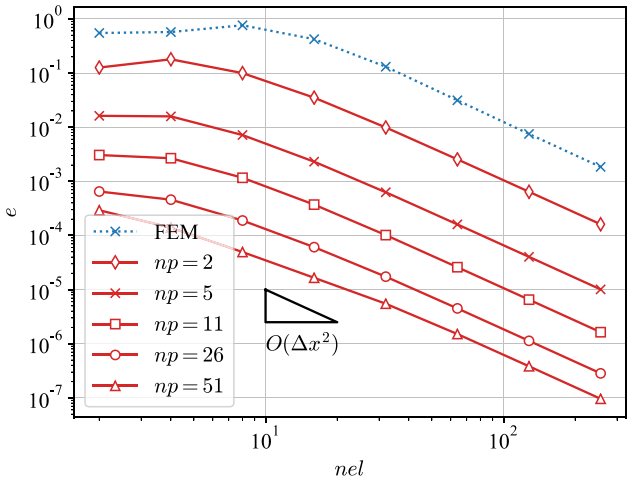

Fig. 10 Advection–diffusion–reaction with an exponential Source. Convergence of the error of P-DNS regarding the choice of *np*

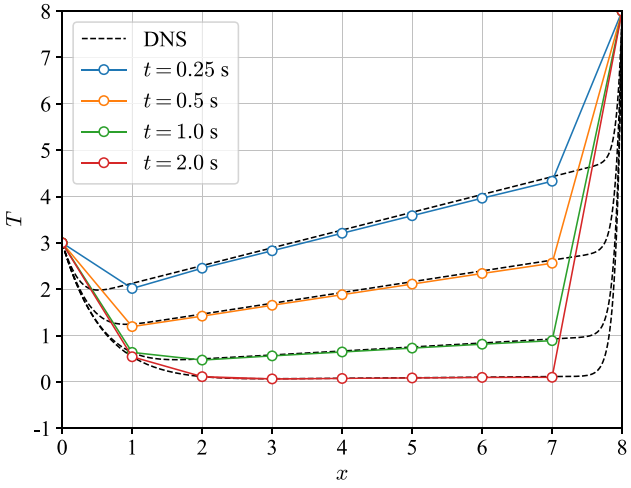

Fig. 11 A transient advective–diffusive–reactive problem. DNS solution is compared with the P-DNS solutions on the nodes of the coarse mesh. Times plotted are 0.25 s, 0.5 s, and 1s. Time step is $\Delta t = 0.125$ s and $\theta = 0.5$

problem on a mesh of 1000 uniform-size linear elements using the standard Galerkin-FEM, a time-step size of 0.005 s, and second-order operators.

Results show that an exponential layer gradually develops at the right boundary which triggers a global instability in the FEM when a coarse mesh is used, see references [15,22]. This global instability is successfully controlled by the P-DNS method.

The convergence rate of the error applying the P-DNS method in transient problems is studied from hereafter. The procedure consists on evaluating the convergence when *nel* is increased while keeping constant $np = 26$ and a CFL = $u\Delta t/\Delta x = 0.25$. Two values for θ parameter are tested: $\theta = 0.5$, the second order *Crank-Nicolson* scheme, and $\theta = 1$, the first order *Euler* scheme. In addition, the errors obtained with FEM and $\theta = 0.5$ are also computed. Figure 12 shows that the P-DNS errors inherits the convergence rate of the temporal discretization used: linear with $\theta = 1$ and almost quadratic with $\theta = 0.5$ (ROC=3.2). This slight detriment of the convergence is due to neglect the contribution of

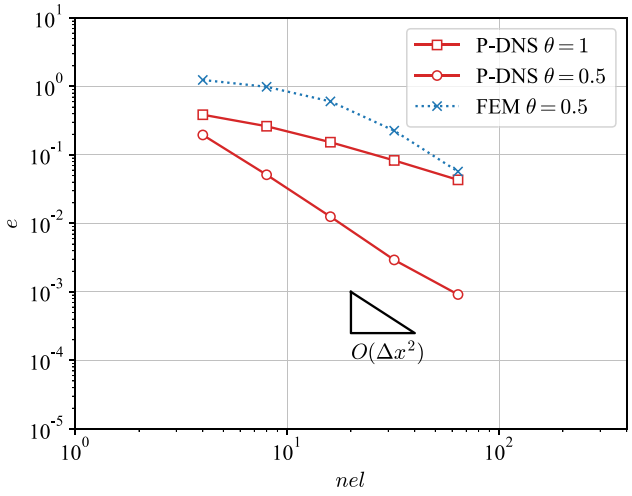

Fig. 12 A transient advective–diffusive–reactive problem. Convergence of the error of P-DNS and FEM solutions when keeping fixed CFL=0.25

the first and second derivatives of T^n to compute $F(x)$ with Eq. (23) when calculating the fine scale contributions from Eqs. (27a) and (27b).

The solutions obtained with FEM with $\theta = 0.5$ show quadratic convergence, but the absolute error for a given *nel* is up to three order larger than the obtained with the P-DNS solutions. In fact, the accuracy of FEM with 128 linear elements can be overcome by P-DNS using only eight, which shows again the capability of the P-DNS method of reducing the number of degrees of freedom.

Arbitrariness of the splitting between the coarse and fine scales

In this test the uniform advection of a temperature field with a constant source term is solved from the initial to the steady state. The problem data is $u = 1, k = 10^{-3}, r = 0$, and $f(x, t) = 1$. The homogeneous boundary condition is imposed at $x = 0$ and $x = L = 1$. The solution develops an exponential layer at the outflow boundary $x = L$. Figure 13 shows snapshots at different simulation times of the DNS solution with 1000 elements and 1000 time steps. The thin boundary layer towards the right wall triggers instabilities that makes impossible to find a solution using non-stabilized approaches with coarser meshes due to the restriction of Pe < 1.

This test aims studying the arbitrariness of the splitting between the coarse and fine scales. Therefore, while the numerical parameters $\theta = 1$ and $\Delta t = 0.05$ are established, the parameters *nel* and *np* are varied but preserving the factor $(nel)(np - 1) = 20$. This keeps constant $h_s = L/((nel)(np - 1)) = 1/20$, the grid step for the discretization of the source. Snapshots of the transient P-DNS solution with $nel = 1$ and $np = 20$ are shown in Fig. 13.

To properly compare the P-DNS solutions with the different choices of *nel* and *np*, the error e_{np} is defined as the root mean square error of the numerical predictions on the location of the source discretization points for each simulated time, i.e.

$$e_{np} = \sqrt{\frac{\sum_{n=1}^{ndt} \sum_{p=1}^{(nel)(np-1)} \left[T(x_p, t^n) - T^{ref}(x_p, t^n)\right]^2}{(nel)(np-1)(ndt)}}, \tag{32}$$

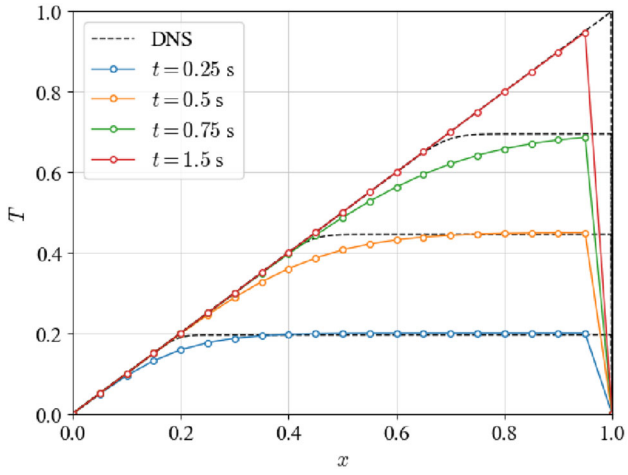

Fig. 13 An advective–diffusive problem with constant source. DNS solutions at times 0.25 s, 0.5 s, 0.75 s, and 1.5 s are compared with P-DNS solution on the *np* points

Table 1 An advective–diffusive problem with constant source

nel	1	2	4	5	10	20
np	21	11	6	5	3	2
e_{np}	0.0181	0.0181	0.0181	0.0181	0.0181	0.0181
E	361	163	91	109	739	6859

The absolute error is evaluated using the temperature field on the discretization points of the source. *E* is an estimation of the computational effort measured as the number of operations per time-step required to solve the equation system and update the source discretization points

where *ndt* is the number of time steps and x_p is the location of a given source discretization point. Table 1 presents e_{np} for the tests performed. The fact that the P-DNS solution does not change confirms the arbitrariness of the selection of *nel* and *np* once established h_s.

A particular choice is considering the coarse mesh composed only by a single 2-nodes element. This split avoids solving an equation system for the coarse mesh. Indeed, obtaining the solution of the current time step relies on the update of the *np* points through Eq. (28). The solution at each discretization point $T(x_p, t^{n+1})$ is decoupled from the current value of any other point. This strategy turns P-DNS to work as an *explicit* solver, but without the standard stability limits of $\text{Fo} = k\Delta t/(2\Delta x^2) < 1$ and $\text{CFL} = u\Delta t/\Delta x < 1$. However, according to Eq. (28), the update of a given point depends on the previous states of the other discretization points to which it shares the element in the coarse mesh. Therefore, the computational effort is now devoted to compute the matrix-vector product of sizes $np \times np$ by $np \times 1$.

The computational effort for the different choices of *nel* and *np* can be estimated. The most expensive tasks are (a) the solution of an equation system of $nel - 1$ unknowns to obtain the updated state on mesh nodes, and (b) computing of *nel* matrix-vector products of size $np - 2$ to update the value on the discretization points inside the elements. Using standard procedures to perform these tasks, it leads to a computational effort *E* of approximately $E = O((nel - 1)^3) + nel \times O((np - 2)^2)$ operations. Table 1 presents the estimated value of *E* for the tests performed in this section, where the minimum is found at $nel = 4$ and $np = 6$. It is well known that the requirements presented for both procedures represent a maximal bound. The number of operations can be decreased using

established algorithms as iterative solutions for sparse matrix systems, while the computation times can be reduced with parallel computing, among many other improvements. However, these studies are left for future work.

Conclusions

To solve a given problem, the P-DNS method arbitrarily divides the unknown into *coarse* and *fine* scales. The final result is obtained as an overlay of both scales.

The main strength of the P-DNS method is that the fine-scale can be solved offline in a non-dimensional way, just once, and lastly applied for any advection reaction diffusion problem. The method relies on isolating and precomputing the most expensive part of the solution, the evaluation of the fine-scale through dimensionless RVEs. Once tabulated the fine-scale outputs, the method allows solving problems with relatively coarse meshes using these non-dimensional results. From this point of view, the method belongs to Reduction Order Models (ROM), in which problems with a few degrees of freedom are solved using previously tabulated coefficients.

Compared to standard ROM like POD or PGD, P-DNS has the advantage of considering the whole structure of the solution. Hence its accuracy and possibility of reduction in problems where there is no separation of variables.

The approximation error of the methodology for one-dimensional transient advective–diffusive–reactive with source problems is numerically shown to quadratically decrease with the grid step for the discretization of the source, h_s. In the practise, we expect a P-DNS' user receives an unique database with a predefined number np of discretization points for the source. Therefore, the user can adjust the accuracy of the solution by refinement of the coarse mesh.

In conclusion, the possibilities of the method seen as a way of reducing the degrees of freedom of a given problem have been shown. The formulation of this method in 1D is sufficient to confirm the strength of this novel approach. This idea could be taken as a basis for future use of reduction methods for more real engineering applications where the separation of variables is often non-existent.

Acknowledgements

The authors acknowledge the financial support from the CERCA programme of the Generalitat de Catalunya, and from the Spanish Ministry of Economy and Competitiveness through the "Severo Ochoa Programme for Centres of Excellence in R&D" (CEX2018-000797-S). The authors also wish to acknowledge CONICET, Universidad Nacional del Litoral and Agencia I+D+i from Argentina for their financial support through grants PICT 2018 N° 03106, PICT-2018 N° 2464, and CAI+D grant number 50620190100132LI.

Special thanks to Profesor Pedro Morin for very useful discussions and for his patience.

Author contributions

SI: theoretical development. JG: implementation, test design, and validation. NN: methodology and conceptualization. All authors read and approved the final manuscript.

Declarations

Competing interests

The authors declare that they have no competing interests.

Received: 27 May 2022 Accepted: 27 September 2022
Published online: 28 October 2022

References

1. Idelsohn SR, Cardona A. Reduction methods and explicit time integration technique in structural dynamics. Advances in Engineering Software. 1984;6(1):36–44.

2. Idelsohn SR, Cardona A. A load-dependent basis for reduced nonlinear structural dynamics. Computers & Structures. 1985;20(1–3):203–10.
3. Cardona A, Idelsohn S. Solution of non-linear thermal transient problems by a reduction method. International journal for numerical methods in engineering. 1986;23(6):1023–42.
4. Baiges J, Codina R, Idelsohn S. Explicit reduced-order models for the stabilized finite element approximation of the incompressible navier-stokes equations. International Journal for Numerical Methods in Fluids. 2013;72(12):1219–43.
5. Cosimo A, Cardona A, Idelsohn S. General treatment of essential boundary conditions in reduced order models for non-linear problems. Advanced Modeling and Simulation in Engineering Sciences. 2016;3(1):1–14.
6. Farhat C, Avery P, Chapman T, Cortial J. Dimensional reduction of nonlinear finite element dynamic models with finite rotations and energy-based mesh sampling and weighting for computational efficiency. International Journal for Numerical Methods in Engineering. 2014;98(9):625–62.
7. Farhat C, Chapman T, Avery P. Structure-preserving, stability, and accuracy properties of the energy-conserving sampling and weighting method for the hyper reduction of nonlinear finite element dynamic models. International journal for numerical methods in engineering. 2015;102(5):1077–110.
8. Ryckelynck D. A priori hyperreduction method: an adaptive approach. Journal of computational physics. 2005;202(1):346–66.
9. Ryckelynck D, Chinesta F, Cueto E, Ammar A. On thea priori model reduction: Overview and recent developments. Archives of Computational methods in Engineering. 2006;13(1):91–128.
10. Nouy A. A priori model reduction through proper generalized decomposition for solving time-dependent partial differential equations. Computer Methods in Applied Mechanics and Engineering. 2010;199(23–24):1603–26.
11. Chinesta F, Ladeveze P, Cueto E. A short review on model order reduction based on proper generalized decomposition. Archives of Computational Methods in Engineering. 2011;18:395–404. https://doi.org/10.1007/s11831-011-9064-7.
12. Chinesta F, Cueto E. Pgd-based modeling of materials, structures and processes. Springer 2014.
13. Chinesta F, Ladevèze P. Separated representations and pgd-based model reduction. Fundamentals and Applications, International Centre for Mechanical Siences, Courses and Lectures. 2014;554:24.
14. Idelsohn S, Nigro N, Larreteguy A, Gimenez JM, Ryzhakov P. A pseudo-dns method for the simulation of incompressible fluid flows with instabilities at different scales. Computational Particle Mechanics. 2020;7(1):19–40.
15. Idelsohn SR, Gimenez JM, Nigro NM, Oñate E. The pseudo-direct numerical simulation method for multi-scale problems in mechanics. Computer Methods in Applied Mechanics and Engineering. 2021;380:113774. https://doi.org/10.1016/j.cma.2021.113774.
16. Gimenez JM, Idelsohn SR, Oñate E, Löhner R. A multiscale approach for the numerical simulation of turbulent flows with droplets. Archives of Computational Methods in Engineering. 2021;28(6):4185–204.
17. Oliver J, Caicedo M, Huespe AE, Hernández JA, Roubin E. Reduced order modeling strategies for computational multiscale fracture. Computer Methods in Applied Mechanics and Engineering. 2017;313:560–95. https://doi.org/10.1016/j.cma.2016.09.039.
18. Allier P, Chamoin L, Ladevèze P. Proper generalized decomposition computational methods on a benchmark problem: introducing a new strategy based on constitutive relation error minimization. Adv. Model. and Simul. in Eng. Sci. 2015;2(17). https://doi.org/10.1186/s40323-015-0038-4
19. Badías A, González D, Alfaro I, Chinesta F, Cueto E. Local proper generalized decomposition. International Journal for Numerical Methods in Engineering. 2017;112(12):1715–32.
20. Cosimo A, Cardona A, Idelsohn S. Improving the k-compressibility of hyper reduced order models with moving sources: applications to welding and phase change problems. Computer Methods in Applied Mechanics and Engineering. 2014;274:237–63.
21. Cosimo A, Cardona A, Idelsohn S. Global-local rom for the solution of parabolic problems with highly concentrated moving sources. Computer Methods in Applied Mechanics and Engineering. 2017;326:739–56.
22. Puigferrat A, de-Pouplana I, Oñate E. FIC-FEM formulation for the multidimensional transient advection-diffusion-absorption equation. Computer Methods in Applied Mechanics and Engineering 2020;365:112984. https://doi.org/10.1016/j.cma.2020.112984

Publisher's Note